Anal. Chem. **1997,** *69,* 490−499

Characterization of a Tunable Optical Parametric Oscillator Laser System for Multielement Flame Laser Excited Atomic Fluorescence Spectrometry of Cobalt, Copper, Lead, Manganese, and Thallium in Buffalo River Sediment

Jack X. Zhou, Xiandeng Hou, Suh-Jen Jane Tsai,† Karl X. Yang, and Robert G. Michel*

Department of Chemistry, University of Connecticut, 215 Glenbrook Road, Storrs, Connecticut 06269-4060

A pulsed (10 Hz) optical parametric oscillator (OPO) laser system based on β-barium borate (BBO) crystals and equipped with a frequency-doubling option (FDO) was characterized for use in laser excited atomic fluorescence spectrometry (LEAFS). This all-solid-state laser has a narrow spectral line width, a wide spectral tuning range (220−2200 nm), and a rapid, computer-controlled slew scan of wavelength (0.250 nm s^{-1} in the visible and infrared, and 0.125 nm s^{-1} in the ultraviolet). The output power characteristics (15−90 mJ/pulse in the visible, 1−40 mJ in the infrared, and 1−11 mJ in the ultraviolet), laser pulse-to-pulse variability (3−13% relative standard deviation, RSD, of the laser pulses), conversion efficiency of the FDO (2−17%), and spectral bandwidth in the visible spectrum (0.1−0.3 cm^{-1}) were measured. The laser was used as the excitation source for a flame LEAFS instrument for which rapid, sequential, multielement analysis was demonstrated by slew scan of the laser. The instrument allowed about 640 measurements to be made in about 6 h, with triplicate measurements of all solutions and aqueous calibration curves, which yielded accurate analyses of a river sediment (National Institute of Standards and Technology, Buffalo River Sediment, 2704) for five elements with precisions <5% RSD. Comparable or improved flame LEAFS detection limits over literature values were obtained for cobalt (2 ng mL^{-1}), copper (2 ng mL^{-1}), lead (0.4 ng mL^{-1}), manganese (0.2 ng mL^{-1}), and thallium (0.9 ng mL^{-1}) by flame LEAFS.

Laser excited atomic fluorescence spectrometry (LEAFS) is an extremely sensitive technique for the determination of the elements in a wide variety of samples. The high-sensitivity results from the high population of excited analyte atoms that can be achieved with a laser, compared to a conventional light source, and the low spectral backgrounds, low incidence of spectral interferences, and low number of matrix interferences. The most sensitive detection limits that have been reported have been as low as a few attograms.[1] It is routinely possible to analyze for femtogram amounts of metals in microliter volumes of sample solution, and often by direct vaporization in a graphite furnace of milligram weights of solid samples or slurried solid samples.[2,3] Compared to a conventional light source, laser excitation also allows nonresonance transitions to be used, which reduces to an unimportant level any laser radiation scattered off the vaporized sample. The low incidence of spectral and matrix interferences ensures that the technique is very selective. The selectivity is further enhanced by the high sensitivity of the technique, because samples can often be diluted to the point where matrix interferences no longer exist, while the sensitivity remains adequate for the analysis. Also, the long linear dynamic range (LDR) of the calibration curves, typically 5−7 orders of magnitude, allows for greater flexibility in sample dilution, which improves the ease of analyses. A critical component in a LEAFS instrument is the laser source itself. The basic requirements for the laser include wavelength tunability across the ultraviolet and visible spectrum to allow for the determination of as many elements as possible, together with high peak energy to enable the atomic energy levels to be optically saturated by the laser, and high average power to allow for maximum signal-to-noise ratio.

Until now, pulsed excimer- or YAG-pumped tunable dye lasers have been used most in LEAFS[4] because they have been the only laser sources with sufficient peak energy and wavelength tunability to allow a wide range of elements to be determined. Unfortunately, dye lasers require a change in an often toxic and flammable dye solution before a wavelength change of more than 10−20 nm can be made. Moreover, dye lasers require 15 or more dyes to cover the entire visible wavelength range. Consequently, a change in element, which normally requires a change in dye, can take anything from a few hours to a few days, depending on any optical alignment or concomitant maintenance that might be necessary. This has meant that LEAFS has never been considered to be a routine sequential multielement technique because it takes too long, and it is too messy, to switch to another element. Dye degradation over time is another disadvantage that causes the laser energy to gradually decrease over a time span that varies between one and a dozen weeks. In general, the poor ruggedness or reliability of dye laser systems and the consequent necessary

† Permanent address: Department of Applied Chemistry, Providence University, 200 Chungchi Rd., Shalu, Taichung, Tsien, 43301, Taiwan, ROC.

(1) Smith, B. W.; Womack, J. B.; Omenetto, N.; Winefordner, J. D. *Appl. Spectrosc.* **1989**, *43*, 873−876.

(2) Butcher, D. J.; Irwin, R. L.; Takahashi, J.; Su, G.; Wei, G. T.; Michel, R. G. *Appl. Spectrosc.* **1990**, *44*, 1521−1533.

(3) Lonardo, R. F.; Yuzefovsky, A. I.; Yang, K. X.; Michel, R. G. *J. Anal. At. Spectrom.* **1996**, *11*, 279−285.

(4) Butcher, D. J.; Dougherty, J. P.; Walton, A. P.; Wei, G. T.; Irwin, R. L.; Michel, R. G. *J. Anal. At. Spectrom.* **1988**, *3*, 1059−1078.

S0003-2700(96)00789-5 CCC: $14.00

high level of technical training of the operator have conspired to prevent the routine application of LEAFS in analytical chemistry.

The search for alternatives to the pulsed dye laser has centered in recent years on solid-state lasers such as the pulsed titanium: sapphire laser.[5] This laser has a wide tuning range from about 700 to 900 nm, which can be frequency doubled into the UV, 350−450 nm, by use of second harmonic generation techniques. This still leaves large gaps in the visible and UV that can be filled only by use of further doubling and mixing techniques,[6] Raman shifting,[7] and/or optical parametric frequency conversion.[8] A laser system based on a titanium:sapphire laser with full tunability throughout the UV and visible is likely to be complex and expensive. Moreover, the cumulative effect of many harmonic generation and Raman shifting steps may well lead to low energies, especially in the deep UV. When these lasers became commercially available, and possibly viable for LEAFS, they were followed almost immediately by the availability of commercial solid-state laser systems based on optical parametric oscillation (OPO), which have the excellent characteristics discussed in the present paper. Consequently, no examples of the use of Ti: sapphire systems in LEAFS have yet been published. It turns out that OPO laser systems have a wider tuning range than Ti: sapphire systems, and it is so easy to tune their wavelength that sequential multielement analysis becomes a feasible proposition. This paper illustrates the use of an OPO with a LEAFS instrument in an example sequential multielement analysis of a river sediment standard reference material.

Principles of Optical Parametric Oscillation. An OPO is an all-solid-state, nonlinear optical conversion device that is based on the parametric interaction between the electrical field of a pump source and a birefringent nonlinear optical material.[9] Although OPO-based laser systems were first demonstrated[10] in 1965, it is only recently that they have become viable as replacements for dye lasers, due to the availability of nonlinear crystals, such as β-barium borate, with good optical properties, high damage threshold, and large nonlinear susceptibility. Unlike conventional lasers, there is no population inversion involved in the parametric frequency conversion process, as it does not depend on any form of atomic or molecular transition. Instead, the electric field in the pump laser directly drives the electrons in the nonlinear optical material. The oscillating electrons respond by generation of linearly and nonlinearly polarized waves determined by the polarizability of the medium. The induced nonlinear polarization couples the energy from the *pump* wave at frequency ω_p into two new tunable frequencies ω_s and ω_i, which are named the *signal* and *idler* waves, respectively. This energy transfer process is done in such a way that energy is conserved as given by

$$\omega_p = \omega_s + \omega_i \tag{1}$$

The spontaneous three-photon parametric process can be represented by analogy with an optically pumped three-level laser,[11] as shown in Figure 1. The upper energy level can be tuned by adjustment of the pump wavelength, ω_p. However, the tuning is normally achieved by adjustment of the middle energy level rather than the pump wave. For a given pump frequency, ω_p, numerous frequency pairs can meet the energy conservation condition, which is the origin of the OPO's tunability. It is the momentum conservation, or phase matching, that governs the process to yield a specific frequency pair:

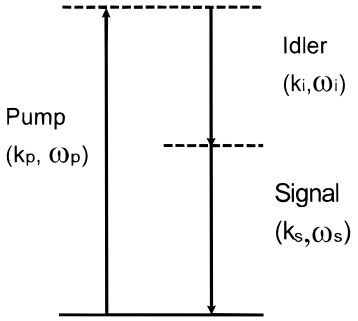

Figure 1. Three-level representation of a three photon parametric process. *k* is the value of the momentum vector of a wave and ω the corresponding frequency of the wave. A high-energy photon, ω_p, from the *pump* wave breaks down into lower energy signal and idler output photons, ω_s and ω_i. The energy levels, in dashed lines, are tunable via creation of phase matching conditions at the middle level and/or at the pump wavelength ω_p for the top level.

$$\mathbf{k}_p = \mathbf{k}_s + \mathbf{k}_i \tag{2}$$

where $\mathbf{k}_p$, $\mathbf{k}_s$, and $\mathbf{k}_i$ are the momentum vectors for pump, signal, and idler waves, respectively.[12] The magnitude of the **k** vector depends on refractive index, with the result that simultaneous satisfaction of both energy and momentum conditions is possible through manipulation of the refractive indexes in a nonlinear, anisotropic medium, such as a β-barium borate (BBO) crystal. The extraordinary wave experiences different refractive indexes, at the same wavelength, when it propagates in different directions with respect to the optic axis. While for an ordinary wave, the index of refraction remains the same as a function of angle of incidence. This 'birefringence" phenomenon is utilized in OPO lasers to compensate for material dispersion so that phase matching can occur throughout the tunable spectral range. Type I phase matching occurs if matching is established when the polarization of the pump is orthogonal to that of the signal and idler waves. Detailed information, and a comparison between collinear and noncollinear pump configurations, can be found in the literature.[13] Wavelength tuning of OPOs can be done via manipulation of either temperature or crystal orientation in order to gain control over the effective refractive index and the magnitude of the **k** vector. A pulsed "free running" OPO without bandwidth restricting optical elements generates a broadband

(5) Moulton, P. F. *J. Opt. Soc. Am. B* **1986**, *3*, 125−133.
(6) Ledingham, K. W. D.; Singhal, R. P. *J. Anal. At. Spectrom.* **1991**, *6*, 73−77.
(7) Funayama, M.; Mukaihara, K.; Morita, H.; Okada, T.; Tomonaga, N.; Izumi, J.; Maeda, M. *Opt. Commun.* **1993**, *102*, 457−460.
(8) Reed, M. K.; Steiner-Shepard, M. K.; Negus, D. K. *Opt. Lett.* **1994**, *19*, 1855−1857.
(9) Byer, R. L. Optical Parametric Oscillators. In *Quantum Electronics: A Treatise*; Rabin, H., Tang, C. L., Eds.; Academic Press: New York, 1975; Vol. 1, Part B.
(10) Giordmaine, J. A.; Miller, R. C. *Phys. Rev. Lett.* **1965**, *14*, 973−976.
(11) Tang, C. L.; Cheng, L. K. *Fundamentals of Optical Parametric Processes and Oscillators*; Letokhov, V. S., Shank, C. V., Shen, Y. R., Walther, H., Eds.; Laser Science and Technology: An International Handbook, Vol. 20; Harwood Academic Publishers: Amsterdam, The Netherlands, 1995.
(12) Yariv, A. *Optical Electronics*, 3rd ed.; CBS College Publishing: New York, 1989.
(13) Gloster, L. A. W.; Jiang, Z. X.; King, T. A. *IEEE J. Quantum Electrom.* **1994**, *30*, 2961−2969.

spectral output of the order of 10 cm^{-1}.[14] To obtain the tunable narrow bandwidth radiation, which is necessary for atomic spectrometry, injection-seeded wavelength control and insertion of intracavity dispersing elements can be used.[15,16]

Optical parametric oscillation can produce wavelengths that are difficult to generate by conventional laser sources simply because the parametric process does not depend on any specific transition in a material. Moreover, the phase matching characteristics and broad wavelength coverage of the available nonlinear optical materials give the OPO a wide wavelength tuning range. Frequency conversion efficiency can also be very high because, unlike conventional three-level lasers, parametric generators respond only to the presence of an input; neither nonradiative nor relaxation processes are involved. In addition, compared with dye lasers, the OPO does not exhibit degradation in the active medium, which gives the potential for maintenance-free operation. Now, fully computer-controlled OPOs are available that have a tuning range that covers 440 nm to 2 μm with pulse energies of the order of hundreds of millijoules.[17] Experience in the present authors' laboratory indicates that these features result in a laser that is versatile, reliable, and easy to use, with a broad tuning range, and with all wavelengths accessible by computer control.

Applications of OPO Laser Systems. In the past few years, various spectroscopic applications with OPO lasers have been demonstrated. Johnson et al.[18] applied a BBO OPO to coherent anti-Stokes Raman spectroscopy (CARS) to obtain rotationally resolved Raman spectra of nitrogen and oxygen in air at various temperatures. Chen[19] has demonstrated the improvement in scan range that can be obtained for CARS instrumentation by use of a narrow line width ($\leq$0.2 cm^{-1}) OPO laser. Kawasaki et al.[20] used a BBO OPO in thermal lens spectrometry for measurement of the thermal lens spectrum of nitrogen dioxide. To the present authors' knowledge, no OPO applications have been reported in atomic spectrometry.

In the work described in the present paper, an OPO laser system was used in a flame LEAFS instrument to determine the concentrations of five elements in a river sediment standard reference material. The determination of heavy metals in sediment is of significant environmental and geological interest. As a result, many sediment analyses by different analytical methods have been reported. Flame atomic absorption spectrometry (flame AAS) has been used by Sinex et al.,[21] Nieuwenhuizw et al.,[22] and others. The determination of copper, nickel, and lead in a sediment sample was not successfully done by Davidson et al.[23] due to the insufficient sensitivity of the flame AAS technique. Electrothermal atomizer atomic absorption spectrometry (ETA-AAS) has been shown to be a much more sensitive approach for the analysis. However, serious matrix interferences on the determination of lead and zinc have been encountered by Carrondo et al.[24] and by Caravajal and Mahan for lead and copper determinations.[25] The same authors encountered severe background signals and multiple peaks that prevented the accurate determination of thallium. Inductively coupled plasma atomic emission spectrometry (ICP-AES) is an alternative that has the advantage of rapid, simultaneous multielement analysis, but it also has the classical disadvantage of spectral interferences. Although good accuracy and precision have been obtained by McLaren et al.,[26] when the methodology was applied to a marine sediment sample, the sensitivity of ICP-AES was found inadequate for some trace metal determinations. Spectral interferences were also a problem, for example in the determination of cadmium.

Flame laser excited atomic fluorescence spectrometry has not been widely used, probably because of the disadvantages associated with dye lasers as well as the advantages of the ICP and graphite furnace over the flame as an atom cell. Nevertheless, the primary objective of the work described here was to explore the ease with which an OPO laser system would allow a sequential multielement analysis rather than to work with any particular atom cell. A chemical flame has a primary advantage that it is very simple to set up and use, and analyses can be done very quickly. Hence, the flame was used in this work as a test case for LEAFS as a sequential multielement technique. However, it is useful to note that flame LEAFS[27−30] has excellent detection limits, high selectivity, and good sequential multielement analytical potential, given a laser that can be scanned rapidly enough. Here, a sequential multielement analysis of a river sediment sample was performed by flame LEAFS with an OPO laser system, after sample preparation by direct acid digestion. In addition, due to the novelty of OPO laser systems, some basic characterization of the laser was done to corroborate the main features claimed by the manufacturers.

EXPERIMENTAL SECTION

Characterization of the OPO Laser System. Figure 2 shows a schematic diagram of the optical parametric oscillator laser system used in this work. Table 1 lists the laser equipment and other equipment that was used to make the various types of measurements described below. Detailed information on the OPO laser can be found in ref 17 but is summarized here. A frequency-tripled Nd:YAG laser, injection-seeded by a laser diode, was used to pump a tunable OPO laser equipped with a frequency doubler. This OPO design uses BBO crystals cut for type I phase matching in the master and power oscillators with a collinear pump configuration. The 355-nm pump energy of typically 540 mJ is partitioned between the two oscillators by use of a dielectric beam splitter that directs approximately 170 mJ into the master oscillator. An intracavity grating set at a grazing incidence is used in the master oscillator to achieve a narrow line width and wide

(14) Haub, J. G.; Hentschel, R. M.; Johnson, M. J.; Orr, B. J. *J. Opt. Soc. Am. B* **1995**, *12*, 2128−2141.
(15) Fix, A.; Schröder, T.; Wallenstein, R. *J. Opt. Soc. Am. B* **1993**, *10*, 1744−1750.
(16) Bosenberg, W. R.; Pelouch, W. S.; Tang, C. L. *Appl. Phys. Lett.* **1989**, *55*, 1952−1954.
(17) Johnson, B. C.; Newell, V. J.; Clark, J. B.; McPhee, E. S. *J. Opt. Soc. Am. B* **1995**, *12*, 2122−2127.
(18) Johnson, M. J.; Haub, J. G.; Barth, H. D.; Orr, B. J. *Opt. Lett.* **1993**, *18*, 441−443.
(19) Chen, P. C. *Anal. Chem.* **1996**, *68*, 3068−3071.
(20) Kawasaki, S.; Lane, R. J.; Tang, C. L. *Appl. Opt.* **1994**, *33*, 992−996.
(21) Sinex, S. A.; Cantillo, A. Y.; Helz, G. R. *Anal. Chem.* **1980**, *52*, 2342−2346.
(22) Nieuwenhuize, J.; Poley-Vos, C. H.; van den Akker, A. H.; van Delft, W. *Analyst* **1991**, *116*, 347−351.
(23) Davidson, C. M.; Thomas, R. P.; McVey, S. E.; Perala, R.; Littlejohn, D.; Ure, A. M. *Anal. Chim. Acta* **1994**, *291*, 277−286.
(24) Carrondo, M. J. T.; Reboredo, F.; Ganho, R. M. B.; Oliveira, J. F. S. *Talanta* **1984**, *31*, 561−564.
(25) Caravajal, G. S.; Mahan, K. I. *Anal. Chim. Acta* **1983**, *147*, 133−150.
(26) McLaren, J. W.; Berman, S. S.; Boyko, V. J.; Russell, D. S. *Anal. Chem.* **1981**, *53*, 1802−1806.
(27) Fraser, L. M.; Winefordner, J. D. *Anal. Chem.* **1972**, *44*, 1444−1451.
(28) Weeks, S. J.; Haraguchi, H.; Winefordner, J. D. *Anal. Chem.* **1978**, *50*, 360−368.
(29) Omenetto, N.; Human, H. G. C.; Cavalli, P.; Rossi, G. *Analyst* **1984**, *109*, 1067−1070.
(30) Walton, A. P.; Wei, G. T.; Liang, Z.; Michel, R. G.; Morris, J. B. *Anal. Chem.* **1991**, *63*, 232−240.

Table 1. Instrumentation

Nd:YAG laser	Spectra Physics (Mountain View, CA), Model GCR-250; injection seeded; repetition rate, 10 Hz; output wavelength (frequency-tripled output beam), 355 nm; pulse duration, 6 ns
OPO laser	Spectra Physics, Model MOPO 730−10; direct *idler* and *signal* output range, 440−2000 nm; frequency-doubled *idler* output wavelength range, 356−1000 nm; frequency-doubled *signal* output range, 220 −345 nm
attenuator	Newport (Irvine, CA), Model 935−3; aperture, 3 × 9 mm; spectral range, 200−2100 nm; attenuation, 0−20 and 2−40 dB for horizontally and vertically polarized beams, respectively
flame apparatus	Perkin-Elmer (Norwalk, CT), air−acetylene premixed burner, 10-cm path length
monochromator	CVI Laser Corp. (Albuquerque, NM), Model DK-240, computer-controlled scanning monochromator; focal length, 240 mm; *f*/3.9; grating, 1200 g mm^{-1}
ellipsoidal mirror	Aero Research Assoc., Inc. (Port Washington, NY), 90° off-axis; diameter, 89 mm; F_1 = 140 mm, $F2$ = 260 mm
boxcar integrator	Stanford Research Systems (Sunnyvale, CA), Models SR250, SR280, and SR275 for integrator, system mainframe, and display modules, respectively; used in last sample mode
photomultiplier	Hamamatsu (Middlesex, NJ), Model R212 UH
preamplifier	LeCroy Corp. (Chestnut Ridge, NY), Model VV100 BTB wide band
joulemeter	Molectron Detector, Inc. (Portland, OR), Model J3−05DW pyroelectric joulemeter
calorimeters	Scientech, Inc. (Boulder, CO), Model 38−2UV5, spectral range, 190−360 nm; time constant, 22 s; and Model 38-0101, spectral range, 400−1200 nm, time constant, 12 s
computer	Gateway 2000 (North Sioux City, SD), Model P5−60
data acquisition board	Data Translation (Marlboro, MA), Model DT2801A; resolution, 12 bit; digitization rate, 27.5 kHz
software	for data acquisition from the boxcar, and control of OPO laser wavelength scan through an RS-232 port on the OPO controller, written in Microsoft Visual Basic 3.0
linear charge-coupled device (CCD) array	CVI Laser Corp. East (Putnam, CT), Model SpectraMatch CCD module; pixel number, 2048; pixel size, 14 μm^2; pixel pitch, 14 μm; digitizer resolution, 10 bit; digitization rate, 330 kHz
étalons	Molectron Corp. (no longer exists), Models DL226-B and DL226-C for the wavelength ranges 440−570 and 560−730 nm, respectively; free spectral range, 1.1 cm^{-1}

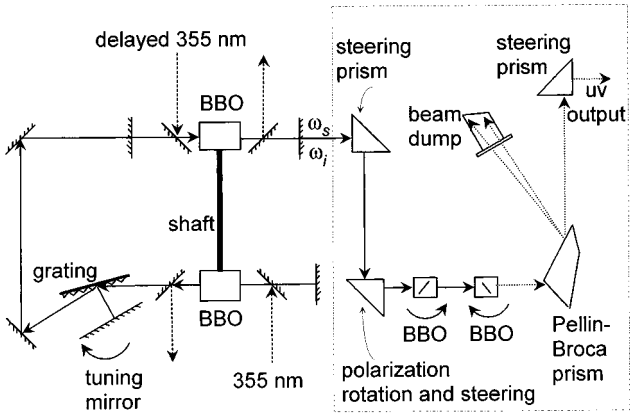

Figure 2. Simplified, schematic diagram of the optical parametric oscillator laser system equipped with frequency doubling. For a full description, see text.

tuning range. The first diffracted order of the signal component is reflected back into the cavity by an aluminized tuning mirror to form a singly resonant cavity for the signal beam. The output from the master oscillator is obtained from the zero-order reflection off the grating, and the signal component is used to injection-seed the power oscillator resonator. An unstable resonator design is used for the power oscillator to provide low beam divergence. About 370 mJ of the 355-nm pump energy is time delayed and then directed into and out of the power oscillator. The master oscillator BBO crystal is mounted on the same shaft as the power oscillator crystal, which, after adjustment for a wavelength match with the master oscillator crystal, allows for the wavelengths of both crystals to be tuned in synchronization. Two BBO crystals cut at 56° and 36° are used in the frequency doubler to cover a wavelength range from below 220 to above 440 nm. The crystals are switched at about 270 nm. Output from the power oscillator is passed into the frequency-doubling BBO crystals by use of beam steering and polarization rotation prisms to satisfy the phase matching requirements of the crystals. Wavelength tuning of the OPO is achieved by computer control of the tuning mirror (Figure 2), together with synchronized rotation of the BBO crystal angles. The two basic modes provided by the manufacturer for the wavelength tuning are "track" and "table", where "track" uses a photodetector that allows the output power to be monitored for feedback to the crystal position, and "table" uses a lookup table to fix the crystal angle. The "table" mode provides greater stability once the correct angle is found.

During the experiments for measurement of the signal and idler beam characteristics at the OPO output, the steering prism at the OPO output was replaced with a dichroic mirror set. The signal and idler beams were separated by the dichroic mirrors to allow them to exit from separate windows. The OPO wavelength was then scanned in steps, under computer control through an RS-232 communication port, while at each wavelength increment the laser power at the output was measured by use of a calorimeter and digitized by the data acquisition system (Table 1). The signal and idler beam power outputs were measured by use of the 38-0101 calorimeter (Table 1) and integrated for 60 s, while the UV radiation was measured by use of the 38-2UV5 calorimeter (Table 1) and integrated for 100 s. A 50% beam splitter was used for measurement of the power of the 355-nm output from the YAG laser. The conversion efficiency of the frequency doubler, expressed as a percentage, was calculated from the ratio of the fundamental and frequency-doubled output pulse energies in millijoules per pulse, or in milliwatts of power.

The pulse-to-pulse variation in the energy of the frequency-tripled output from the YAG (at 355 nm) as well as the signal, idler, and frequency-doubled outputs of the OPO were measured with a joulemeter (Table 1). A small portion of the corresponding radiation was taken to the joulemeter by use of a beam splitter. The voltage output from the joulemeter was fed to a boxcar through a delay line of about 70 ns. The data acquisition system was externally triggered by the "busy" signal from the boxcar, which was used in its "last sample" mode. This mode provides the average signal during the last open gate and allows the signal size that results from each laser pulse to be measured. A total of 150 pulses were collected for calculation of pulse-to-pulse variation at each wavelength that was measured.

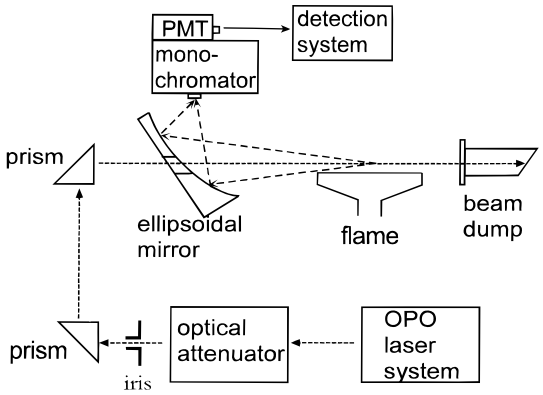

Figure 3. Block diagram of the OPO-based flame LEAFS experimental arrangement. See text.

The signal beam spectral line width was characterized with Fabry−Perot interferometry[31] by use of interference fringes recorded on a linear charge-coupled device (CCD) array (Table 1), with a typical integration time of between 250 and 350 ms. The interferograms were, therefore, the average of two or three fringes due to the 100-ms (10-Hz) duty cycle of the laser. The fringes were formed by an étalon and imaged with a biconvex lens of 30-cm focal length onto the CCD array. For the wavelength range of 450−680 nm, two étalons were required. All the étalons employed had a free spectral range (FSR) of 1.1 cm^{-1}. The laser spectral bandwidth, L, in inverse centimeters, at the measurement wavelength λ (nm) was approximated to be

$$L = (D_2/D_{1,3})\mathrm{FSR} \qquad (3)$$

where $D_{1,3}$ is half the distance between the first and the third interference fringes, or rings, D_2 is the full width at half-maximum (fwhm) at the second ring, and the free spectral range, FSR, of the étalon is given in inverse centimeters.

Flame LEAFS Instrumentation. A diagram of the flame LEAFS arrangement[4] used in the present work is shown in Figure 3 with the major instrumental components in Table 1. An 89-mm-diameter, 90° off-axis ellipsoidal mirror (F_1 = 140 mm and F_2 = 260 mm), with a 6-mm-diameter hole in the center, through which the OPO laser beam was passed, was positioned in front of a flame at an angle of 45° with respect to the excitation axis. The flame was a standard, long-path atomic absorption burner. A variable optical attenuator was inserted into the laser path to control the excitation energy. The excitation laser beam from the OPO had an approximately circular diameter of 7 mm that passed through the attenuator, which had 3-mm × 7-mm entrance and exit apertures. The long axis was then reduced to 6 mm at an iris (Figure 3) before it passed through a 6-mm hole in the mirror that was used to collect the fluorescence at 180° to the direction of the laser beam. The attenuator was orientated in such a way that the excitation laser beam was aligned with its long axis (6 mm) parallel to the upward flame direction. The fluorescence was focused onto the entrance slit of a quarter-meter monochromator (f/3.9), with a typical slit width of 0.5 mm. The detection system consisted of a photomultiplier tube (PMT), a preamplifier, a 70-ns delay line, a boxcar integrator used with a 50-ns gate and its "last sample" mode, and a computer-based data acquisition system. The boxcar was triggered by the YAG laser radiation through an optical fiber and a PMT (not shown in the diagram). All the fluorescence signals were integrated for 10 s unless otherwise stated. Cobalt, copper, lead, manganese, sodium, and thallium were excited at 304.400, 324.754, 283.306, 279.482, 588.995, and 276.787 nm, respectively. The frequency-doubled laser energies for excitation were 15 μJ/pulse for copper, lead, manganese, and thallium, and 20 μJ/pulse for cobalt. For sodium excitation, the fundamental OPO signal output was attenuated to 15 μJ/pulse. For cobalt, copper, lead, manganese, sodium, and thallium, fluorescence was detected at 340.5, 510.5, 405.8, 403.3, 589.6, and 352.9 nm, respectively.

Reagents. Aqueous standards and sample solutions were prepared on a class 100 (U.S. Federal 209b) clean bench. Subboiled deionized water and ultrapure acids (Baker Inc., Jackson, TN) were used. Cobalt, copper, lead, manganese, sodium, and thallium stock solutions were prepared from cobalt powder, copper, lead metal, manganese flake, sodium chloride (HiPure grade, Spex Industries, Metuchen, NJ), and thallium(I) nitrate (Puratonic grade, Alfa Products, Danvers, MA) dissolved in a minimum volume of concentrated nitric. A stock solution of 5% lanthanum, for use as a releasing agent solution, was prepared by dissolution of lanthanum chloride (HiPure grade, Spex Industries, Metuchen, NJ) in water. Aqueous standard solutions of cobalt, lead, manganese, sodium, and thallium were made by serial dilution to a final volume of 100 mL that contained 2% nitric acid and 0.5% lanthanum chloride. Copper and sodium stock solutions were diluted with 2% nitric acid only. A 2% solution of nitric acid and a solution of 2% nitric acid plus 0.5% lanthanum chloride served as the blanks for the analytes of copper and sodium and of other analytes, respectively. All glassware and plasticware was soaked in 20% nitric acid (Reagent grade, Baker Inc.) for 24 h and then rinsed with subboiled deionized water prior to use.

Sample Preparation. Buffalo River sediment standard reference material (SRM 2704) was obtained from the National Institute of Standards and Technology (NIST, Gaithersburg, MD). Multiple 1.00-g dried sediment samples were weighed into Polytetrafluoroethylene (PTFE) beakers, to which were added 10 mL of hydrochloric acid, 3 mL of nitric acid, and 10 mL of hydrofluoric acid. The solutions were heated at 60−80 °C for several hours to dryness. The addition of acids and evaporation were repeated three times, followed by the addition of a minimum amount of hydrochloric acid to dissolve the residue. The solution was then transferred to a 100-mL plastic volumetric flask. A small amount of residue remained at this point which was rinsed several times with water, and the resultant solution was combined with the previous solution. Nitric acid was added to the digested sample so that the final acid concentration was approximately 2% (v/v). Lanthanum chloride was added to the sample solution to a final concentration of 0.5% for the determination of cobalt, lead, manganese, and thallium. Lanthanum chloride was not used for the determination of copper.

Analytical Procedures. An air−acetylene flame was used with gas flow rates that were about 1.4 L min^{-1} acetylene and 5.2 L min^{-1} air. Most measurements were performed under slightly fuel-rich flame conditions, as indicated by visual adjustment of the flame until the fuel-rich yellow color was just visible. The atomic fluorescence signals were maximized by optimization of the burner height with respect to the laser beam and appropriate alignment of the optical axis of the monochromator. It turned

(31) Morris, M. B.; Mcllrath, T. *J. Appl. Opt.* **1979**, *18*, 4145−4151.

out that lack of proper synchronization of the rotation of the Pellin−Broca prism with the rotation of the frequency-doubling crystals (Figure 2) can lead to beam wander away from the optical axis of the flame LEAFS instrument. The beam pointing position was adjusted for several wavelength positions, by use of alignment procedures in the laser's manual, and the resultant "look-up" table was stored in the laser's controller system to minimize the beam pointing error throughout the wavelength tuning range of 220−345 nm. If this procedure was not done, the beam wandered during a wavelength scan by several millimeters from the optimum position in the flame.

The OPO wavelength calibration accuracy was found by the use of known atomic lines. The OPO output was scanned through the known atomic excitation wavelengths to find the maximum fluorescence signal. Five elements, thallium, lead, manganese, cobalt, and copper, were chosen for the experiment, which covered a wavelength range from 276.787 to 324.754 nm. The difference between the wavelength on the readout on the OPO controller at the wavelength that gave the peak fluorescence signal, and the known value of the wavelength from tables, reflected the OPO calibration accuracy. Excitation scans were done at a scan rate of 0.025 nm s^{-1} in a continuous scan mode for the construction of spectra. The wavelength reading on the OPO that gave the maximum intensity on repeated sodium excitation profiles was used to assess the OPO calibration repeatability.

Fluorescence signals produced by samples or standards were integrated for 10 s for each element at each of their fluorescence lines, followed by subtraction of a blank. Calibration graphs were constructed with aqueous standards that contained lanthanum chloride for all elements except copper and across a concentration range of at least 3 orders of magnitude. The concentration detection limits were obtained by extrapolation of the analytical calibration curves to a concentration equivalent to a signal-to-noise ratio of 3. The lowest point on the calibration curve was within a factor of 10 of the detection limit. The noise level was determined by the standard deviation of 16 measurements of the blank at a wavelength 50 pm away from the corresponding analytical line.

RESULTS AND DISCUSSION

There were two primary aims of the work described here. The first was to characterize operating characteristics and corroborate the specifications of this new type of laser, while the second was to test whether or not the operational convenience of being able to tune the laser to any wavelength throughout a wide wavelength range would result in a capability for sequential multielement analysis by LEAFS, with a flame as a convenient example atom cell.

YAG and OPO Output Power Characteristics. The output power of the YAG pump laser was measured to be about 5.4 W, or 540 mJ/pulse, at 355 nm. For the data presented here, the YAG pump power was between 4.6 and 5.4 W. Typically, the flash lamps in the YAG laser lasted about 4 months of 40 h weeks, but the energy of the YAG output was not the primary indicator of the necessity for replacement of the flash lamps. The primary indicator was the spectral line width of the laser, which eventually widened to the point where the sensitivity of the LEAFS measurements was affected by more than a factor of 10. The manufacturers of the laser indicated that the age of the flash lamps affects the spatial intensity distribution of energy in the YAG beam to the point where it affects the parametric oscillation process, the energy at the output, and the spectral line width. No studies were promulgated to correlate the flash lamp energy with the parametric oscillation process or the laser spectral line width, because a loss of sensitivity of the LEAFS measurements turned out to be the best operational indicator of the necessity for flash lamp replacement. Before the loss in spectral line width, but near the end of the lifetime of the flash lamps, which corresponded to a loss in energy of the YAG below about 4−4.5 W, the OPO stopped oscillating at a gradually increasing number of wavelengths. Sometimes the oscillation could be restarted by tweaking the alignment of the BBO crystals and other optics at a particular wavelength. Nevertheless, during the 4 months of normal operation of the laser, optical realignment was not done, and only slight and simple adjustments of one or two key optical or electronic components were necessary once every couple of weeks.

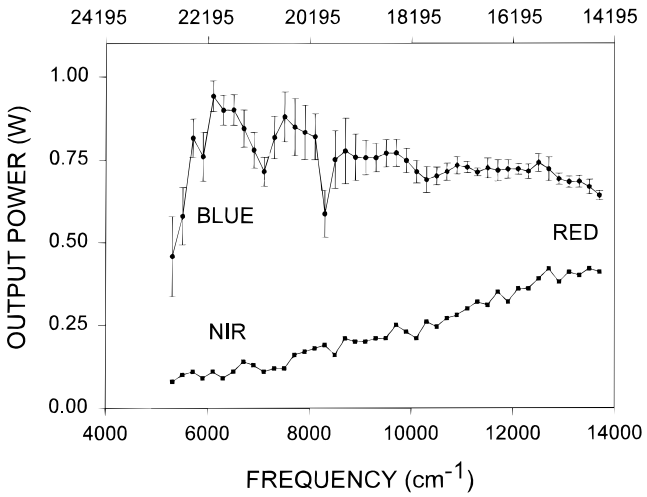

Figure 4. Average output power of the optical parametric oscillator laser system, signal (●) and idler (■) radiation vs frequency, with the top and bottom axes for signal and idler beams, respectively. One watt of output power corresponds to a pulse energy of about 100 mJ. Units of inverse centimeters were used for the frequency axis to allow both signal and idler to be plotted on the same graph simultaneously, although the laser's wavelength was calibrated in nanometers. The frequency increment was 200 cm^{-1}. The error bars on the signal power graph represent the long-term power stability of the laser and are the minimum and maximum powers of four scans obtained during the course of 6 days. The mean of the four scans was plotted.

The results of measurements of signal and idler beam output power vs frequency are shown in Figure 4, which was the result of four scans done over 6 days. Over 500 mW of average signal power (35−90 mJ/pulse) in the visible, and 100 mW of idler power (1−40 mJ/pulse) in the near-infrared, were routinely achievable. The output power was fairly flat over the measurement region. A warm-up time of about 2 h was necessary before the best short-term stability in the output power, within a range of ±5%, was achievable for a 12-h day. Inclusion of the power changes during the first 2 h gave a variation in power up to a factor of 2 worse. Over a longer term of several days, the general trend was a drop in power with time. The long-term signal output power stability is illustrated by the error bars in Figure 4, which represent the range of power that was measured at each wavelength, with the graph drawn through the middle of the range. No optical adjustment was done during the 6 days of the experiment, and all the scans were taken after at least 2 h of warm-up. The day-to-day differences between the maximum and minimum signal

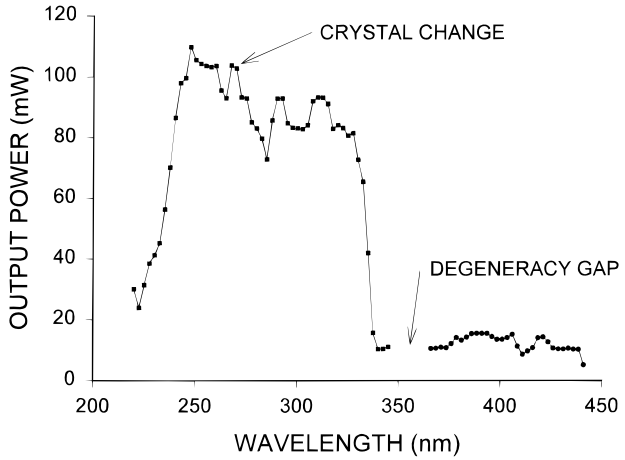

Figure 5. Output power for the frequency-doubled radiation in the wavelength range from 220 to 441 nm. Two crystals cut for 56° and 36° were used to cover the measured output range. The gap between 345 and 366 nm was due to the degeneracy of the OPO laser at this wavelength. The first part of the curve (■) was the frequency-doubled output obtained by use of the signal beam, while the second part (●) was obtained by use of the idler beam.

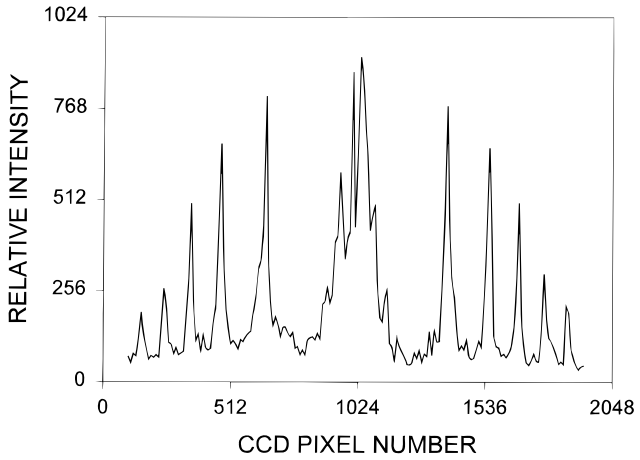

Figure 6. Interference fringes recorded at 500 nm with a linear CCD array. The integration time was such that the average of two or three consecutive interferograms was recorded. The calculated laser spectral line width was about 0.2 cm^{-1}.

output powers were more noticeable around 440 nm, where the variation was up to ±15%, but overall the laser was stable in output energy at most wavelengths with variations between ±2% and ±10%. The variations became greater after 10 days of operation, by a factor of almost 2, but slight optical adjustments were usually adequate to bring back the power. The laser was stable over its specified operating range of between 440 and 680 nm. It was also found that the laser was able to maintain lasing down to 420 nm, but with a poorer stability of about ±30%. Since the signal and idler outputs are generated by the same parametric process, it was assumed that the idler would exhibit similar error bars. Accordingly, no measurements were made of the long-term stability of the idler beam. Since the data in Figure 4 were gathered, some new optical mounts have been installed in the laser which might improve some of the stability figures, but no such data are yet available.

The frequency-doubled output power in the wavelength range 220−441 nm was measured as shown in Figure 5, in which the wavelength increment was 2.5 nm. At 270 nm, a change automatically occurred in the system from a frequency-doubling BBO crystal cut at 56° to a crystal cut at 36°. However, the points at 270.0 and 272.5 nm were directly connected on the graph. The gap between 345 and 366 nm was due to the degeneracy of the OPO fundamental signal and idler beams. Measurement of the frequency-doubled output to the red side of 441 nm was not attempted since the choice of fundamental signal or idler beam was a more reasonable option to cover that wavelength region. The output power in the ultraviolet was of the order of tens to hundreds of milliwatts (1−11 mJ/pulse), which was sufficient for LEAFS and most atomic spectroscopic applications. The efficiency calculation for the frequency doubler was based on Figures 4 and 5, and gave the highest conversion efficiency of about 17% when the signal frequencies were doubled, and the lowest of about 1% when the idler frequencies were doubled.

Relative Standard Deviation of Laser Output Pulse Energies. The relative standard deviation of the output of the YAG laser is reflected in the output of the optical parametric oscillation, which may result in poor pulse-to-pulse stability at the output of the laser system. The YAG pump laser in the present experiment was able to provide 355-nm pump radiation with a relative standard deviation (RSD) of individual laser pulses of typically 1.6%. The RSDs of the signal, idler, and frequency-doubled outputs were measured for most of the wavelength ranges between 220 and 2200 nm. A typical RSD value in the ultraviolet was found to be around 3−5%, although in certain regions, such as around 220−270 nm, it was as high as 6−13%. In the visible and infrared, the RSD was also in the 3−5% region, with poorer RSD at extremes of operation of the signal and idler beams, of 6−12% in the blue (440−490 nm), and in the infrared near 2000 nm (1400−2000 nm). These relative standard deviations are rather similar to, or perhaps a little better than, those found with modern excimer- and YAG-pumped dye laser systems.

Signal Spectral Line Width Characteristics. Figure 6 shows a typical set of interference fringes recorded for a laser line width measurement at 500 nm, from the fundamental OPO signal output, and represents a calculated bandwidth of 0.2 cm^{-1}. The interferogram indicated that laser mode hopping over a short period of time was not noticeable. However, multipeak interference fringes, broadened by as much as 50%, were observed when a larger averaging time was used at the CCD, which indicated mode hopping of the laser. The line width of the signal radiation was measured as a function of wavelength in 5-nm increments. A spectral line width between 0.1 and 0.25 cm^{-1} was measured throughout the signal wavelength range of 460−690 nm. Measurement of the spectral line width of the idler and frequency-doubled output was not possible due to the limited number of étalons on hand, although it can be assumed that the line width of the frequency-doubled radiation was within a factor of 2 of the line width of the signal's line width. In LEAFS, a spectral line width of 3−10 pm is usually desired to ensure a high signal-to-noise ratio. A spectral line width that extends outside the collisionally broadened spectral profile of the absorption line contains unabsorbable stray radiation that increases background stray light and degrades the signal-to-noise ratio. Based on the above measurements of the OPO signal line width, the spectral bandwidth of the frequency-doubled output of the OPO laser system was probably ≤20 pm, depending on the wavelength, which is about 50−100% wider than those of many dye lasers, especially those equipped with an intracavity étalon. This appeared to be an acceptable line width for most LEAFS measure-

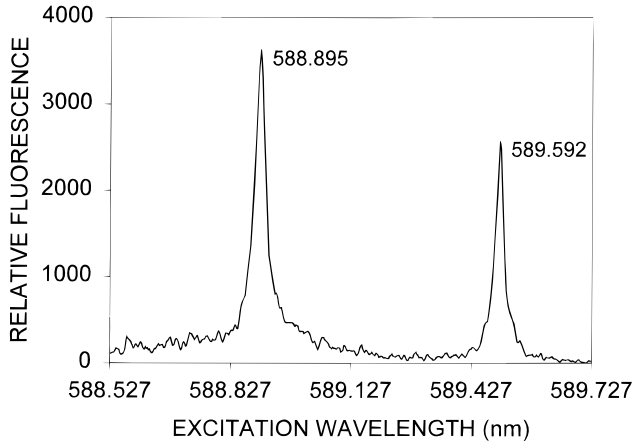

Figure 7. Spectrum of the sodium D lines. The spectrum was obtained in continuous scan mode at a scan rate of 0.025 nm s^{-1}.

ments, as measured signal-to-noise ratios were found to be comparable to past work of the present authors, after allowance had been made for the rather low, 10-Hz repetition rate of the OPO laser system compared to the 500-Hz excimer-pumped dye laser systems used in the past.

Calibration Accuracy and Temperature Stability. The OPO calibration accuracy was measured by peaking the laser at the known atomic excitation lines of five elements and comparing the known wavelength with the wavelength on the readout of the OPO laser system controller. The average deviation of the readout from the known wavelength was about 17 pm, which was about the spectral line width of the laser. A repeatability of 5 pm was determined from repeated sodium excitation scans. A representative sodium excitation spectrum at the D lines is shown in Figure 7, which was obtained in "continuous scan" mode at a scan rate of 0.025 nm s^{-1}. The total time required for the complete scan was 48 s.

The OPO laser system was found to be sensitive to environmental temperature changes in the laboratory, which meant that, as the temperature changed, the laser would lose optical alignment in ways that were not clear, but which resulted in an increase in spectral line width at the output. A temperature change of greater than ±2.5 °C was enough to cause this problem. However, a temperature range of 5 °C was not difficult to control in the laboratory. It appears that the temperature of the room in the middle of the operating range was probably the temperature at which the OPO laser system was optically aligned at the immediate prior service of the laser. To return the laser back to optical alignment, it was sufficient to return the room to within the original temperature range, without physical realignment of the optics.

Flame LEAFS Analytical Performance with the Slew Scanned OPO Laser System. One of the primary advantages of an OPO laser system is that it can be rapidly tuned between wavelengths over a very wide wavelength region from the ultraviolet to the near-infrared. For example, to move from the thallium excitation line at 276.787 nm to the copper line at 324.754 nm took the OPO a single command and less than 7 min to change wavelength. When a crystal change was involved for a wavelength range that included the 270-nm point, an additional time of less than 5 min was needed for a switch between the crystals. There were two possible modes of tuning the laser. The first was a continuous scan that was used to obtain the spectrum of the sodium D lines (Figure 7). The D lines were scanned at a rate of 0.025 nm s^{-1}, which was the preferred scan rate found by experiment to ensure that the laser servo system would maintain the necessary wavelength accuracy throughout the scanned wavelength range. Hence, Figure 7 represents a full spectrum around the D lines. It was possible to scan the laser at a faster rate, 0.25 nm s^{-1} for signal and idler, or 0.125 nm s^{-1} for the frequency-doubled output, in a "goto" or slew scan mode that allowed the laser to be sent to the next atomic wavelength, without concern about whether or not the laser was lasing or calibrated during the scan. The reproducibility of this slew scan mode to find the new wavelength was about ±2.5 pm. The aim of the following analytical experiments was to test the ability of the laser system to be used in a slew scan mode to hop from wavelength to wavelength and allow a rapid sequential multielement analysis.

Table 2. Detection Limits (ng mL^{-1}) by OPO Flame LEAFS and Other Techniques

				flame LEAFS	
element	ETA-AAS[a]	FAA[a]	ICP-AES[a]	literature[b]	this work[g]
Tl	0.1	6	2	0.8[c] (1−50 Hz, 1.8−9 s)	0.9
Mn	0.2	1	0.9	0.4[d] (20 Hz, 0.5−5 s)	0.2
Pb	0.1	1	0.4	0.2[e] (1−10 Hz, 1.3 s)	0.4
Co	0.5	10	20	200[f] (1−30 Hz, NA)	2.0
Cu	1	9	40	1.0[d] (20 Hz, 0.5−5 s)	2.0

[a] Reference 32. A 10 μL sample injection volume was assumed for LOD calculations for ETA-AAS. [b] Laser repetition rate, detection time constant. [c] Reference 33. [d] Reference 28. [e] Reference 29. [f] Reference 27. [g] Laser repetition rate, 10 Hz; detection integration time, 10 s.

The experimental setup was first optimized with respect to optical alignment in the flame, ellipsoidal mirror, and laser beam, followed by optimization of the required saturation energy for each element in aqueous solution, and measurement of calibration curves and detection limits for each element to ensure proper overall operation of the instrumentation. Analytical calibration curves were constructed for five elements; thallium, manganese, lead, cobalt, and copper.

To understand the significance of the above optimization, it must be realized that, even given a smoothly operating dye laser system, the present authors have never been able to do five elements sequentially, except over a period of several months, because the difficulties in dye changes provided barriers that were not usually surmountable unless the authors were very determined and very sure that all required data had been collected at the first wavelength. This was a disincentive to change elements more than once every few months. With the OPO laser, the analytical methods for five elements were all optimized in a matter of 2 or 3 weeks. Once the method development and optimizations had been done, it was possible to do the analysis of river sediment for five elements in about 4.5 h, as detailed later.

The detection limits obtained for flame LEAFS excited by the OPO laser system and those obtained by use of other laser systems in the literature are summarized in Table 2. For comparison purposes, the detection limits for these five elements by electrothermal atomization atomic absorption spectrophotometry ETA AAS, flame AAS, and ICP-AES are listed. The detection

(32) *The Guide to Techniques and Applications of Atomic Spectrometry*; Perkin-Elmer: Norwalk, CT, 1990.
(33) Human, H. G. C.; Omenetto, N.; Cavalli, P.; Rossi, G. *Spectrochim. Acta, Part B* **1984**, *39*, 1345−1363.

Table 3. Sequential Multielement Analysis by OPO Flame LEAFS for an Aqueous Multielement Solution

element	amount of analyte in solution (ng mL^{-1}) known	measured[a] ± SD (RSD, %)[b]
Tl	200	201 ± 4 (2)
Mn	500	498 ± 10 (2)
Pb	200	205 ± 5 (2)[a]
Co	500	511 ± 10 (2)
Cu	500	508 ± 4 (1)

[a] The number of sample runs used for the calculation of the standard deviation was three ($n = 3$). [b] SD (RSD, %): standard deviation (relative standard deviation, %).

Table 4. Sequential Multielement Analysis by OPO Flame LEAFS for SRM 2704 River Sediment

element	amount of analyte in the sample (μg g^{-1}) certified	measured[a] ± SD (RSD, %)[b]
Tl	1.2 ± 0.2	1.1 ± 0.04 (3.9)
Mn	555 ± 19	560 ± 21 (3.8)
Pb	161 ± 17	164 ± 2 (1.0)
Co	14.0 ± 0.6	13.1 ± 0.2 (1.3)
Cu	98.6 ± 5.0	90.1 ± 2.9 (3.2)

[a] The number of sample runs used for the calculation of the standard deviation was three ($n = 3$). [b] SD (RSD, %): standard deviation (relative standard deviation, %).

limits in this work were comparable with dye laser excited flame LEAFS reported in the literature, although an improvement of 2 orders of magnitude in the detection limit was achieved for cobalt compared to the literature. Detection sensitivity in flame LEAFS was superior to both ICP-AES and flame AAS for these elements, while the detection limits were comparable or only slightly worse than those possible with ETA-AAS.

After optimization of the OPO beam pointing position throughout the working wavelength range as described in the Experimental Section, the detection limits for the five elements were remeasured, but in a sequential multielement mode. No experimental parameters were adjusted during the experiment, except for the changes in wavelength and control of the energy of the laser beam by use of the attenuator. A total of over 600 measurements were made in about 6 h for construction of five calibration curves, including three measurements for each data point, seven data points, two on-line blanks, and 16 off-line blanks for each calibration curve, with three calibration curves for each element, and total of five elements. An average speed of about 40 s/measurement was achieved. The RSDs for the three measurements at each data point were below 5%, and typically 3%. Deteriorations in signal-to-noise ratios by about an order of magnitude were observed for three of the elements, thallium, manganese, and copper, in the multielement mode compared to the optimized single-element mode (Table 2). This was attributed to laser beam pointing error that remained across the wavelength region. Sufficiently high detection power was still demonstrated in the sequential multielement mode to allow for analysis of the river sediment. Sequential multielement analysis with an aqueous standard multielement solution was then performed to provide a baseline of the expected accuracy and precision for the multielement analysis. The above aqueous standard solutions were used for the determination of each of the five elements in the laboratory-prepared multielement solution. The analytical results are listed in Table 3. High accuracy was achieved, according to Student's *t* test at the 95% confidence level, and better than 5% RSD was achieved for the three measurements of each element. A releasing agent, lanthanum chloride, was added to the calibration standards and the multielement standard solutions for all elements except copper.

Real Sample Analysis Performance. The real sample multielement analysis was done in the same manner as described above. About 400 measurements were made in 4.5 h, including aqueous calibrations, on-line blanks, and sample solutions. The excellent selectivity associated with the multielement flame LEAFS technique allowed the analysis of the NIST river sediment standard reference material (SRM 2704). This was done without spectral interferences, although it was necessary to add a releasing agent, lanthanum chloride, to the standards and sample solutions for all the elements, except copper, in order to obtain accurate analyses. According to Student's *t* test at the 95% confidence level, accurate results were obtained for multielement analysis in the SRM 2704 reference material, as shown in Table 4. A second sample dilution by a further factor of 2 was used for the determination of lead and manganese, which were present in high concentrations in the sample. It was found that some reduction occurred in the signal from these analytes in the river sediment solution compared to the aqueous calibration curve. The matrix may have caused a prefilter effect, which attenuated the excitation radiation.[4] As a result, the atomic transition was not saturated, and the signal declined from the aqueous calibration curve. It was possible to use a higher excitation energy to overcome this situation, as there was enough energy available from the OPO, but dilution was more simple to do. A change in laser energy requires a fairly time-consuming reoptimization to ensure that too much energy is not being used that might degrade the signal-to-noise ratio. In retrospect, it would have been more appropriate to do the saturation studies on a real sample solution rather than on aqueous standards. Exploratory tests did indicate that an increase in excitation energy by a factor of about 6−10 was probably necessary for these two elements, but no further studies were done to define this drop in signal.

CONCLUSIONS

There are two significant differences between the all-solid-state optical parametric laser system used here and an excimer- or YAG-pumped dye laser system. The most significant is the computer-controlled and facile tuning between wavelengths of the OPO. It is this feature that allows sequential multielement analysis to be done by flame LEAFS, which cannot be done with a dye laser. This paper illustrates such an analysis done trivially by the OPO laser system. Although only five elements were determined sequentially here, there is really no upper limit to the number of elements that can be done sequentially, except those limits imposed by the use of any particular atom cell. A flame was chosen here for convenience and ease of use, but, in principle, any other atom cell could be used for LEAFS. The second difference is in the repetition rate of the laser. The present authors have been using an excimer-pumped dye laser, operated at 500 Hz, that has given a predictable and reliable factor of 7 improvement in detection limits compared to a repetition rate of 10 Hz. This means that all the detection limits reported in the present paper could be improved by higher repetition rates. YAG

lasers with higher repetition rates that are suitable to pump an OPO would be an important advance, especially for transient atom cells such as the graphite furnace.

The OPO laser system that was used here has operated very reliably in the authors' laboratory for the last 13 months and can be considered to be virtually a "turn key" system. About every 4 months of 40 h weeks, the YAG laser requires new flash lamps that need rather careful installation and subsequent alignment in the OPO laser. It is possible to damage the expensive BBO crystals by misalignment of the OPO laser. In addition, care in the alignment is necessary to ensure that the OPO lases throughout its wavelength range. After the installation of the flash lamps, very slight adjustments to the optical alignment electronics are required every couple of weeks. The only other significant problem is that the room temperature needs to be controlled to within a 5-deg range, although this is not unduly burdensome. This reliability and facility of use is a major advance in tunable laser technology that can provide major benefits in the productivity of laser-based spectroscopy and analytical chemistry.

The OPO laser had high energy throughout the wavelength range. The energies obtained were so high that the authors used a manual optical attenuator to tune the energy for saturation of the atomic energy levels. Computer-controllable optical attenuators are available with a wide operating wavelength range and offer the possibility that both energy and wavelength can be placed under programmable control, which allows for the concept of a fully automated, sequential, multielement LEAFS instrument. Extension of the wavelength range below 220 nm, by various frequency mixing techniques, is presently being developed in the authors' laboratory to determine whether some of the facile wavelength tuning advantages of the OPO might make mixing a routine proposition for analytical measurements of those elements that require deep ultraviolet radiation.

The degraded signal-to-noise ratio that was observed during the sequential multielement analysis was most likely due to residual laser spatial pointing errors between wavelengths. This is likely to be capable of further optimization by the user, or refinement in design by the manufacturer. There is no intrinsic reason why sequential multielement LEAFS should have poorer detection limits than single-element LEAFS.

Compared with ETA-AAS, flame AAS, and ICP-AES, flame LEAFS gave a rapid, simple, and sensitive sequential multielement analysis. The simplicity and sensitivity of the analysis arose out of the high selectivity, low, correctable matrix interferences, and very low background signals. These features resulted in simple sample preparation procedures, while the rapidity of the analysis arose from the new type of laser and the characteristics of the flame as an atom cell.

ACKNOWLEDGMENT

The optical parametric oscillator laser system was purchased with funds provided by Connecticut Innovations, Inc., under Grant No. 93H030. Some of the remaining equipment was purchased with funds under National Institutes of Health Grant No. GM 32002. Perkin-Elmer Corp. partially supported X.H. with a fellowship. This work was presented in part at the XXII Annual FACSS Conference, Cincinnati, OH, October 15−20, 1995, paper 098; at the 34th Eastern Analytical Symposium and Exposition, Somerset, NJ, November 12−17, 1995, paper 390; and at the 47th Pittsburgh Conference, Chicago, IL, March 3−8, 1996, paper 591.

Received for review August 5, 1996. Accepted November 19, 1996.[⊗]

AC960789P

[⊗] Abstract published in *Advance ACS Abstracts,* January 1, 1997.